862 *Chem. Mater.* **2011,** *23,* 862–873
DOI:10.1021/cm102165r

CHEMISTRY OF MATERIALS
Article

Near-Infrared Solid-State Emitters Based on Isophorone: Synthesis, Crystal Structure and Spectroscopic Properties.†

Julien Massin, Wissam Dayoub, Jean-Christophe Mulatier, Christophe Aronica, Yann Bretonnière,* and Chantal Andraud*

Université de Lyon, Laboratoire de Chimie de l'ENS Lyon, UMR 5182 CNRS-ENS Lyon, 46 allée d'Italie, 69364 Lyon, France

Received August 1, 2010. Revised Manuscript Received November 8, 2010

A series of near-infrared solid-state emitters based on the dicyanoisophorone electron acceptor group was synthesized. The solid-state spectroscopic properties were studied by UV−visible absorption spectroscopy and fluorescence spectroscopy and analyzed in light of the single crystal structures obtained by X-ray diffraction. This series of push−pull dipolar fluorophores differing only by the substituent groups on the donor end display interesting solid-state emission properties on crystal with an emission in the near-infrared ranging from 710 to 790 nm. The origin of the emission depends on the nature of the substituent groups that influence the crystal packing and trigger the formation of long chain of emitting aggregates.

Introduction

Solid-state emissive fluorophores are of fundamental interest because of the multiple potential applications in material sciences and optoelectronic, especially light-emitting diodes (OLEDs)[1] or fluorescent sensors.[2] Recent reports highlighted the use of fluorescent nanocrystals of small organic molecules for interesting applications in biology and bioimaging, such as DNA biochips[3] or sensors for the analysis of biomolecules.[4] Fluorescent nanocrystals contain a high number of molecules resulting in a strong increase of absorption properties and therefore to ultrabrilliant objects exhibiting much higher photostability than isolated dissolved molecules.[5] The crystal structure also favors the delocalization of the fluorescence excitation leading to unique fluorescent transmitters behavior.[6] Such properties greatly enhance the fluorescence contrast over the biological media thus lowering the thresholds of detection. By comparison to their inorganic counterparts crystals based on small organic molecules offer large diversity in chemical composition or functionality and thus physical properties. When biological applications are targeted, long wavelength fluorescence in the red or the near-infrared is highly desirable, as it should provide better spectral separation from medium autofluorescence than both yellow or green fluorescence, and less scattering in turbid media. However, only a few of these objects exhibit strong fluorescence, as organic compounds emitting in the solid-state are limited and red fluorophores even rarer. Most organic fluorophores exhibiting high fluorescence in dilute solutions lose this property in the solid state as a consequence of the tight molecular packing in the crystalline state or amorphous solid phase (thin film) that usually leads to significant molecular interactions and self-quenching particularly if the Stokes shift is small. With few exceptions, organic red or near-infrared emitting fluorophores[1d,7] are flat molecules with extended π-conjugation or strong dipolar donor−acceptor push−pull molecules and therefore prone to aggregation and fluorescence quenching in the solid-state. The most obvious way to restore the fluorescence is to prevent the molecular packing or the $\pi-\pi$-stacking by introducing bulky spacer groups at the periphery of the fluorophores.[8] This approach has proved successful even for

† Accepted as part of the "Special Issue on π-Functional Materials".
*Corresponding author. E-mail: chantal.andraud@ens-lyon.fr.

(1) (a) Veinot, J. G. C.; Marks, T. J. *Acc. Chem. Res.* **2005**, *38*, 632. (b) Chou, P.-T.; Chi, Y. *Chem.--Eur. J.* **2007**, *13*, 380–395. (c) Mitschke, U.; Bäuerle, P. *J. Mater. Chem.* **2000**, *10*, 1471. (d) Chen, C.-T. *Chem. Mater.* **2004**, *16*(23), 4389.
(2) (a) Prasanna de Silva, A.; Gunaratne, H. Q. N.; Gunnlaugsson, T.; Huxley, A. J. M.; McCoy, C. P.; Rademacher, J. T.; Rice, T. E. *Chem. Rev.* **1997**, *97*(5), 1515. (b) Thomas, S. W., III; Joly, G. D.; Swager, T. M. *Chem. Rev.* **2007**, *107*(4), 1339. (c) Basabe-Desmonts, L.; Reinhoudt, D. N.; Crego-Calama, M. *Chem. Soc. Rev.* **2007**, *36*, 993.
(3) (a) Zhao, X.; Tapec-Dytioco, R.; Tan, W. *J. Am. Chem. Soc.* **2003**, *125*(38), 11474. (b) Dubuisson, E.; Monnier, V.; Sanz-Menez, N.; Boury, B.; Usson, Y.; Pansu, R. B.; Ibanez, A. *Nanotechnology* **2009**, *20*(31), 315301.
(4) (a) Wang, L.; Wang, L.; Dong, L.; Bian, G.; Xia, T.; Chen, H. *Spectrochim. Acta, Part A* **2005**, *61*(1−2), 129. (b) Jinshui, L.; Lun, W.; Feng, G.; Yongxing, L.; Yun, W. *Anal. Bioanal. Chem.* **2003**, *377*, 346. (c) Chan, C. P.-y.; Tzang, L. C.-h.; Sin, K.-k.; Ji, S.-l.; Cheung, K.-y.; Tam, T.-k.; Yang, M. M.-s.; Renneberg, R.; Seydack, M. *Anal. Chim. Acta* **2007**, *584*, 7. (d) Sabella, S.; Brunetti, V.; Vecchio, G.; Della Torre, A.; Rinaldi, R.; Cingolani, R.; Pompa, P. P. *Nanoscale Res. Lett.* **2009**, *4*, 1222.
(5) (a) Kim, H. Y.; Bjorklund, T. G.; Lim, S.-H.; Bardeen, C. J. *Langmuir* **2003**, *19*(9), 3941. (b) Sanz, N.; Ibanez, A.; Morel, Y.; Baldeck, P. L. *Appl. Phys. Lett.* **2001**, *78*(17), 2569.
(6) Botzung-Appert, E.; Monnier, V.; Duong, T. H.; Pansu, R.; Ibanez, A. *Chem. Mater.* **2004**, *16*(9), 1609.
(7) Qian, G.; Wang, Z. Y. *Chem.—Asian J.* **2010**, *5*(5), 1006.

 Published on Web 12/13/2010 © 2010 American Chemical Society

Chart 1. Solid-State Red Emitters Based on Dicyanoisophorone

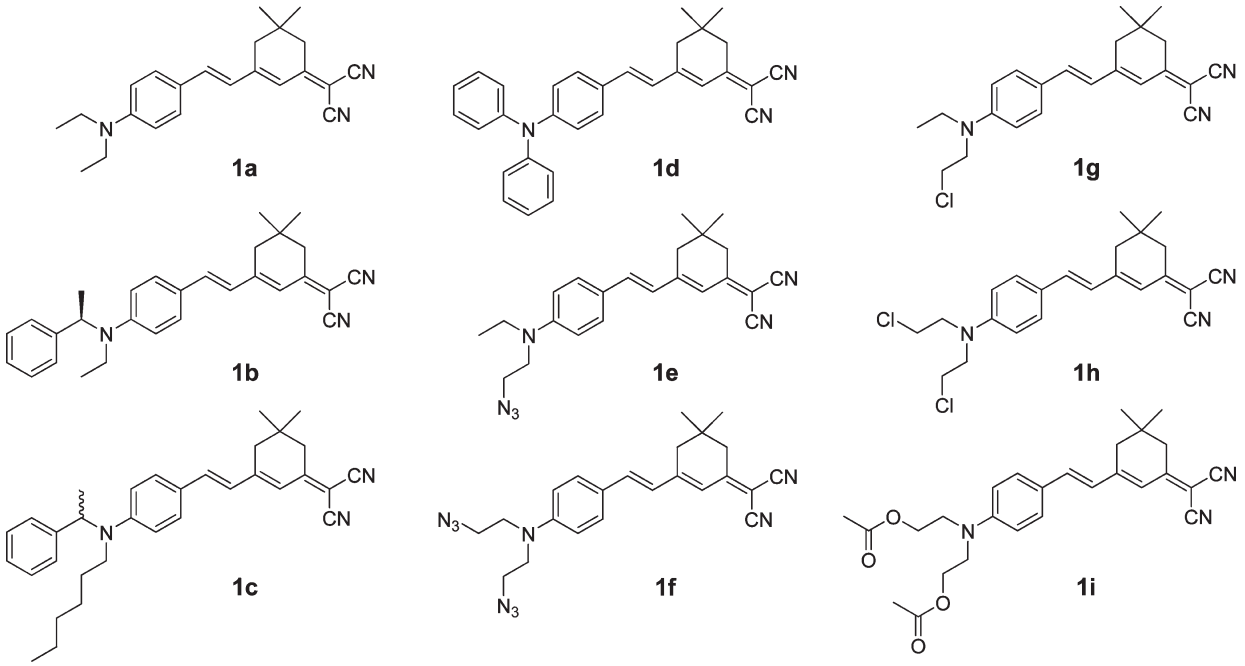

molecules with small Stokes shifts such as BODIPY.[9] Less intuitively, some molecules show unique enhanced emission rather than a fluorescence quenching upon aggregation in the solid state. The origin of the aggregation-induced emission (AIE) and of the aggregation-induced emission enhancement (AIEE) is likely related to the effects of intramolecular planarization or restricted intramolecular vibrational and rotational motions in the solid state or of specific aggregation (H- or J-aggregation) or certainly a combination of all those effects.[10] Following these rules of thumb, large number of AIE/AIEE-active dyes have since been developed,[10d,e] examples of which include red-emitting compounds[10c,11] AIE molecules display high quantum yields in the solid-state and some of them, mostly tetraphenylethenes, have been used as fluorescent probes for biological assays and bioimaging.[12]

During the course of our studies on the use of push−pull chromophores based on the 2-(3,5,5-trimethylcyclohex-2-enylidene)malononitrile or dicyanoisophorone acceptor group for second-order electro-optic materials,[13] we observed that all the crystalline compounds we synthesized bearing this structure were fluorescent in the solid-state. This is hardly surprising as the parent compounds (*E*)-2-(3-(4-(diethylamino)styryl)-5,5-dimethylcyclohex-2-enylidene)-malononitrile and the *N*,*N*-diphenyl analogue were previously described as interesting red emitters for OLEDs.[14]

(8) (a) Englert, B. C.; Smith, M. D.; Hardcastle, K. I.; Bunz, U. H. F. *Macromolecules* **2004**, *37*(22), 8212. (b) Ooyama, Y.; Yoshikawa, S.; Watanabe, S.; Yoshida, K. *Org. Biomol. Chem.* **2006**, *4*, 3406. (c) Lee, Y.-T.; Chiang, C.-L.; Chen, C.-T. *Chem. Commun.* **2008**, No. 2, 217. (d) Kitamura, C.; Tsukuda, H.; Yoneda, A.; Kawase, T.; Kobayashi, T.; Naito, H. *Eur. J. Org. Chem.* **2010**, 3033. (e) Zhou, Y.; Kim, J. W.; Kim, M. J.; Son, W.-J.; Han, S. J.; Kim, H. N.; Han, S.; Kim, Y.; Lee, C.; Kim, S.-J.; Kim, D. H.; Kim, J.-J.; Yoon, J. *Org. Lett.* **2010**, *12*(6), 1272. (f) Kitamura, C.; Matsumoto, C.; Yoneda, A.; Kobayashi, T.; Naito, H.; Komatsu, T. *Eur. J. Org. Chem.* **2010**, 2571.

(9) Ozdemir, T.; Atilgan, S.; Kutuk, I.; Serdar Yildirim, S.; Tulek, A.; Bayindir, M.; Akkaya, E. U. *Org. Lett.* **2009**, *11*(10), 2105.

(10) (a) Luo, J.; Xie, Z.; Lam, J. W. Y.; Cheng, L.; Chen, H.; Qiu, C.; Kwok, H. S.; Zhan, X.; Liu, Y.; Zhu, D.; Tang, B. Z. *Chem. Commun.* **2001**, No. 18, 1740. (b) An, B.-K.; Kwon, S.-K.; Jung, S.-D.; Park, S. Y. *J. Am. Chem. Soc.* **2002**, *124*(48), 14410. (c) Ferrer, M. L.; del Monte, F. *J. Phys. Chem. B* **2005**, *109*(1), 80. (d) Hong, Y.; Lam, J. W. Y.; Tang, B. Z. *Chem. Commun.* **2009**, 4332. (e) Liu, J.; Lam, J. W. Y.; Tang, B. Z. *J. Inorg. Organomet. Polym. Mater.* **2009**, *19*, 249.

(11) (a) Wakamiya, A.; Mori, K.; Yamaguchi, S. *Angew. Chem., Int. Ed.* **2007**, *46*, 4273. (b) Hu, R.; Lager, E.; Aguilar-Aguilar, A.; Liu, J.; Lam, J. W. Y.; Sung, H. H. Y.; Williams, I. D.; Zhong, Y.; Wong, K. S.; Peña-Cabrera, E.; Tang, B. Z. *J. Phys. Chem. C* **2009**, *113* (36), 15845. (c) Liu, Y.; Tao, X.; Wang, F.; Dang, X.; Zou, D.; Ren, Y.; Jiang, M. *J. Phys. Chem. C* **2008**, *112*(10), 3975. (d) Xu, J.; Liu, X.; Lv, J.; Zhu, M.; Huang, C.; Zhou, W.; Yin, X.; Liu, H.; Li, Y.; Ye, J. *Langmuir* **2008**, *24*(8), 4231. (e) Ning, Z.; Chen, Z.; Zhang, Q.; Yan, Y.; Qian, S.; Cao, Y.; Tian, H. *Adv. Funct. Mater.* **2007**, *17*(18), 3799. (f) Tong, H.; Dong, Y.; Häussler, M.; Hong, Y.; Lam, J. W. Y.; Sung, H. H.-Y.; Williams, I. D.; Kwok, H. S.; Tang, B. Z. *Chem. Phys. Lett.* **2006**, *428*(4−6), 326. (g) Yan, W.; Wan, X.; Chen, Y. *J. Mol. Struct.* **2010**, *968*, 85. (h) Palayangoda, S. S.; Cai, X.; Adhikari, R. M.; Neckers, D. C. *Org. Lett.* **2008**, *10*(2), 281.

(12) (a) Wang, M.; Zhang, G.; Zhang, D.; Zhu, D.; Tang, B. Z. *J. Mater. Chem.* **2010**, *20*, 1858. (b) Tong, H.; Hong, Y.; Dong, Y.; Häussler, M.; Li, Z.; Lam, J. W. Y.; Dong, Y.; Sung, H. H.-Y.; Williams, I. D.; Tang, B. Z. *J. Phys. Chem. B* **2007**, *111*(40), 11817. (c) Hong, Y.; Häussler, M.; Lam, J. W. Y.; Li, Z.; Sin, K. K.; Dong, Y.; Tong, H.; Liu, J.; Qin, A.; Renneberg, R.; Tang, B. Z. *Chem.—Eur. J.* **2008**, No. 14, 6428. (d) Dong, Y.; Lam, J. W. Y.; Qin, A.; Li, Z.; Liu, J.; Sun, J.; Dong, Y.; Tang, B. Z. *Chem. Phys. Lett.* **2007**, *446*(1−2), 124. (e) Tong, H.; Hong, Y.; Dong, Y.; Häussler, M.; Lam, J. W. Y.; Li, Z.; Guo, Z.; Guo, Z.; Tang, B. Z. *Chem. Commun.* **2006**, 3705. (f) Chen, Q.; Bian, N.; Cao, C.; Qiu, X.-L.; Qi, A.-D.; Han, B.-H. *Chem. Commun.* **2010**, *46*, 4067. (g) Chen, X.-t.; Xiang, Y.; Li, N.; Song, P.-S.; Tong, A.-j. *Analyst* **2010**, *135*, 1098. (h) Xue, W.; Zhang, G.; Zhang, D.; Zhu, D. *Org. Lett.* **2010**, *12*(10), 2274. (i) Lu, H.; Xu, B.; Dong, Y.; Chen, F.; Li, Y.; Li, Z.; He, J.; Li, H.; Tian, W. *Langmuir* **2010**, *26*(9), 6838. (j) Peng, L.; Zhang, G.; Zhang, D.; Xiang, J.; Zhao, R.; Wang, Y.; Zhu, D. *Org. Lett.* **2009**, *11*(17), 4014. (k) Wang, M.; Zhang, D.; Zhang, G.; Tang, Y.; Wang, S.; Zhu, D. *Anal. Chem.* **2008**, *80*(16), 6443. (l) Wu, W.-C.; Chen, C.-Y.; Tian, Y.; Jang, S.-H.; Hong, Y.; Liu, Y.; Hu, R.; Tang, B. Z.; Lee, Y.-T.; Chen, C.-T.; Chen, W.-C.; Jen, A. K.-Y. *Adv. Funct. Mater.* **2010**, *20*(9), 1413. (m) Liu, Y.; Yu, Y.; Lam, J. W. Y.; Hong, Y.; Faisal, M.; Yuan, W. Z.; Tang, B. Z. *Chem.--Eur. J.* **2010**, *16*(28), 8433. (n) Huang, J.; Wang, M.; Zhou, Y.; Weng, X.; Shuai, L.; Zhou, X.; Zhang, D. *Bioorg. Med. Chem.* **2009**, *17*(22), 7743. (o) Sanji, T.; Shiraishi, K.; Nakamura, M.; Tanaka, M. *Chem.—Asian J.* **2010**, *5*(4), 817.

Scheme 1. Synthesis of fluorophores 1a−1i[a]

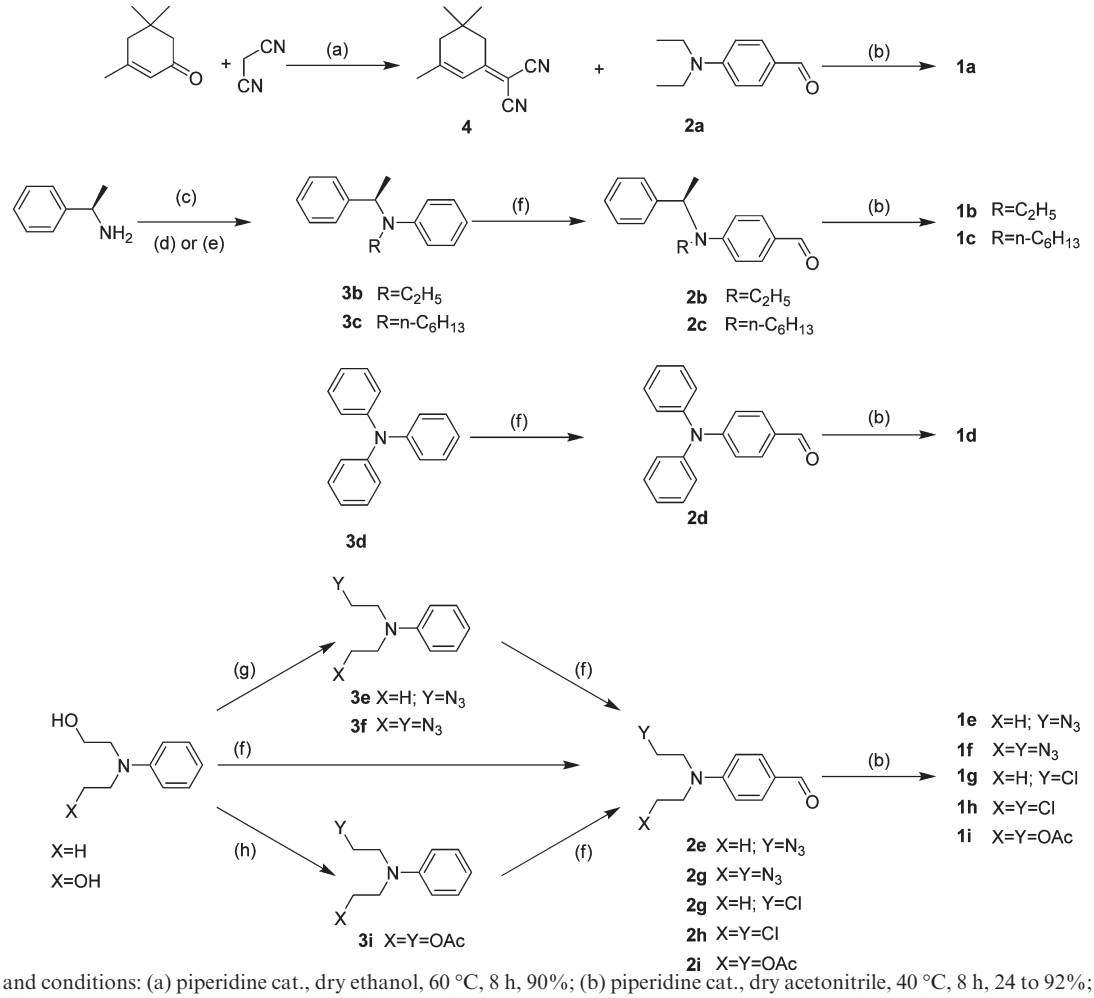

[a] Reagents and conditions: (a) piperidine cat., dry ethanol, 60 °C, 8 h, 90%; (b) piperidine cat., dry acetonitrile, 40 °C, 8 h, 24 to 92%; iodobenzene, CuI cat., L-proline cat., K_2CO_3, dry DMSO, 80 °C, 20 h, 80%; (d) EtI, Na_2CO_3, dry DMF, 65 °C, 3d, 80%; (e) bromohexane, NaI, Na_2CO_3, dry DMF, 95 °C, 20 h, 75%; (f) $POCl_3$, dry DMF, r.t. or 40 °C, 3 to 8 h, 83 to 98%; (g) MsCl, Et_3N, Et_2O, 0 °C, 1 h then NaN_3, DMSO, 80 °C, 3 h, 94 to 96% for the two steps; (h) ref 16.

Nevertheless, those two compounds were the sole examples reported and the solid-state fluorescence properties were not further analyzed, nor were their solid-state structures. We present here the easy obtaining, the solution fluorescent properties as well as the crystal structure and the solid-state fluorescence properties of a series of (*E*)-2-(3-(4-(disubstituted)-amino)styryl)-5,5-dimethylcyclohex-2-enylidene)malononitrile derivatives. All the solid state emitters (compounds **1a**−**i**, Chart 1) bear exactly the same core based on 2-(3,5,5-trimethylcyclohex-2-enylidene)malononitrile but differ by the substituent groups borne by the N donor atom: diethylamino- (**1a**), ethyl(1-phenylethyl)amino- (**1b**), hexyl(1-phenylethyl)amino- (**1c**), diphenylamino- (**1d**), (2-ethyl(1-phenylethyl)amino)ethylamino- (**1e**), di-(2-ethyl(1-phenylethyl)-amino)amino- (**1f**), (2-chloroethyl)ethylamino- (**1g**), di-(2-chloroethyl)amino- (**1h**) and di(acetoxyethyl)amino- (**1i**). Given that such highly dipolar compounds are prone to aggregation,[13] it seemed interesting to us to know the influence of the small structural variation on the molecular packing and the crystal fluorescence properties.

Synthesis. All compounds were obtained starting from isophorone, malononitrile and the corresponding 4-(*N*,*N*-disubstituted)aminobenzaldhyde by a double Knoevenagel reaction sequence. The original procedure was first described by Lemke in 1974[15] doing the two-condensation one-pot in DMF and using a mixture of piperidine, acetic acid, and acetic anhydride as catalyst. This works well for the simpler compound **1a**, but higher yields were obtained by a two-pot sequence isolating the intermediate 2-(3,5,5-trimethylcyclohex-2-enylidene)malononitrile **4** and using dry acetonitrile instead of DMF and only piperidine as a catalyst for the second Knoevenagel condensation (Scheme 1). Amino benzaldehyde were either commercially available (**2a**) or synthesized starting from *N*,*N*-disubstituted aniline via a Vilsmeier−Haack reaction with phosphorus oxychloride and dry DMF.

4-(Diphenylamino)benzaldehyde **2d**, 4-((2-chloroethyl)-(ethyl)amino)benzaldehyde **2g** and 4-(bis(2-chloroethyl)-amino)benzaldehyde **2h** were thus obtained directly from

(13) Rau, I.; Armatys, P.; Chollet, P.-A.; Kajzar, F.; Bretonnière, Y.; Andraud, C. *Chem. Phys. Lett.* **2007**, *442*, 329.

(14) (a) Li, J.; Liu, D.; Hong, Z.; Tong, S.; Wang, P.; Ma, C.; Lengyel, O.; Lee, C.-S.; Kwong, H.-L.; Lee, S. *Chem. Mater.* **2003**, *15*(7), 1486. (b) Yang, L.; Guan, M.; Nie, D.; Lou, B.; Liu, Z.; Bian, Z.; Bian, J.; Huang, C. *Opt. Mater.* **2007**, *29*, 1672.

(15) Lemke, R. *Synthesis* **1974**, *5*, 359.

Table 1. Spectroscopic Properties in Dichloromethane Solution[a]

	λ_{max} (nm)	ε (λ_{max}) (mM^{-1} cm^{-1})	λ_{em}[b] (nm)	$\Delta\tilde{\nu}^{s}$ (cm^{-1})	Φ_F[c] (%)	s (cm^{-1})	V′ (Å^3)
1a	514	40881	658	4257	10	8092	514
1b	509	30104	658	4448	13	8194	619[e]
1c	508	15969	657	4464	12	9224	980
1d	489	23541	690	5957	20 (21[d])	17103	690
1e	492	28909	643	4773	7	7677	562
1f	477	19077	632	5141	4	8300	578
1g	490	24467	643	4856	6	7400	524
1h	473	25578	623	5020	4	10778	554
1i	484	23349	636	4937	5	9110	646

[a] Maxima of linear absorption λ_{max} and of steady-state fluorescence emission λ_{em}, molar absorption coefficients ε at λ_{max} (±20%), Stokes shift $\Delta\tilde{\nu}$, quantum yields of fluorescence Φ_F (±10%), solvatochromic slopes s derived from the fit of the Stoke shift vs Δf using the Lippert−Mataga model and assumed molecular volume V' (see text). [b] λ_{exc} = 490 nm. [c] Standard: rubrene in methanol (Φ_F = 27%).[20] [d] See ref 14a. [e] $V' = \frac{1}{2} \times \frac{V}{Z}$

commercial triphenylamine **3d**, *N*-ethyl-*N*-hydroxyethylaniline **3g** and *N*-phenyldiethanolamine **3h**, respectively. Starting from **3g** and **3h**, the azido and diazido aniline derivatives **2e** and **2f** and the diacetate compound **2i** were obtained by mesylation of the hydroxyl group followed by substitution with sodium azide in DMSO or acetylation with acetic anhydride as described.[16] Vilsmeier−Haack formylation then afforded the benzaldehyde **3e** and **3f** in excellent yields. The enantiopure (*R*)-*N*-ethyl-*N*-(1-phenylethyl)aniline (**3b**) and the racemic (±)-*N*-hexyl-*N*-(1-phenylethyl)aniline (**3c**) were obtained by *N*-arylation of (*R*)-α-methylbenzylamine and (±)-α-methylbenzylamine with iodobenzene catalyzed by L-proline and copper(I) as described by Ma *et al.*[17] followed by alkylation. Vilsmeier−Haack formylation then afforded the corresponding benzaldehyde **2b** and **2c** in excellent yields without racemization.

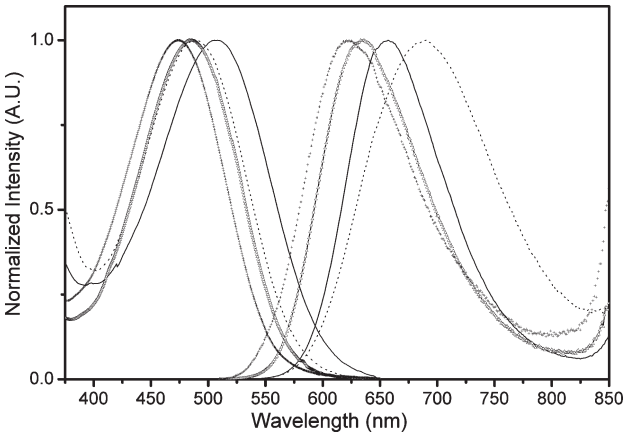

Figure 1. Absorption and fluorescence spectra (λ_{exc} = 515 nm) of **1c** (—), **1d** (· · · ·), **1h** (+), and **1i** (Δ), in dilute dichloromethane solution.

Optical Properties

Solution Properties. The optical properties of all fluorophores were measured in dilute solutions in various solvents. Relevant photophysical data are reported in Table 1. Absorbance and normalized photoluminescence spectra of the representative compounds **1c**, **1d**, **1h**, and **1i** measured at room temperature are shown in Figure 1. Spectra of other compounds are displayed in Figures S1 and S2 in the Supporting Information. All spectra are characterized by a strong and broad structureless absorption band in the visible ranging (in dichloromethane) from 474 nm for **1h** to 514 nm for **1a**. Upon excitation at 525 nm, a broad red emission is observed in dichloromethane, with a shift from 622 nm for **1h** to 692 nm for **1d**.

These bands are characteristic of induced charge transfer (ICT) transitions in push−pull dipolar molecules. In agreement with this attribution and in agreement with previous observations in this type of molecules,[18] these bands present a positive solvatochromism in absorption, weaker than in emission, as shown for **1c** in Figure 2; Figures S3−S10 in the Supporting Information display

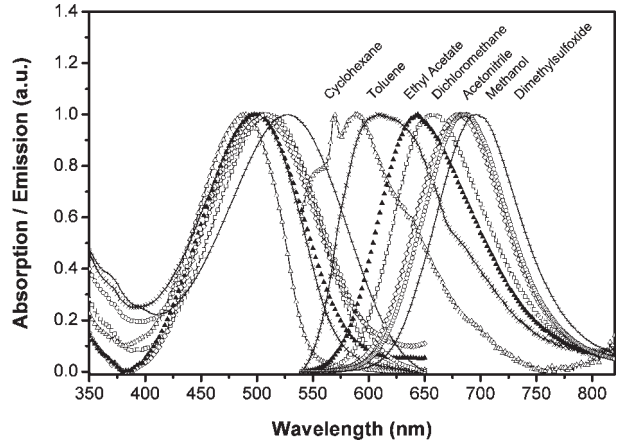

Figure 2. Absorption and emission spectra of **1c** in various solvents: cylohexane (open triangle), toluene (cross), ethyl acetate (closed triangle), dichloromethane (open square), acetonitrile (diamond-shaped), methanol (open circle), and DMSO (dash).

solvatochromism properties of all other chromophores. These positive solvatochromism properties can be analyzed following the Lippert-Mataga model and the solvent polarity parameter, defined by the factor Δf according to eq 1, in which ε and n are the dielectric constant and the refractive index of the solvent, respectively.

The Stokes shift $\Delta\tilde{\nu}$, expressed in cm^{-1}, is expressed as a function of Δf following relationship 2, where K is a constant, c and h are the light speed and the Planck

(16) Wang, N. P.; Leslie, T. M.; Wang, S.; Kowel, S. T. *Chem. Mater.* **1995**, *7*(1), 185.
(17) Ma, D.; Cai, Q.; Zhang, H. *Org. Lett.* **2003**, *5*(14), 2453.
(18) Barsu, C.; Fortrie, R.; Nowika, K.; Baldeck, P. L.; Vial, J.-C.; Barsella, A.; Fort, A.; Hissler, M.; Bretonnière, Y.; Maury, O.; Andraud, C. *Chem. Commun.* **2006**, *45*, 4744.

constant, a is the radius of the spherical cavity of the solute, and $\Delta\mu$ the dipole moment difference between the ground and the excited states.

$$\Delta f = \frac{\varepsilon - 1}{2\varepsilon + 1} - \frac{n^2 - 1}{2n^2 + 1} \quad (1)$$

$$\Delta\bar{\nu} = \frac{2}{hc}\,\Delta f\,\frac{\Delta\mu^2}{a^3} + K \quad (2)$$

Rather good linear correlations were found for all compounds **1a**−**i** (see Figures S11 and S12 in the Supporting Information). The solvatochromism slopes s derived from the Lippert-Mataga model are reported in Table 1; values of s between 7400 and 17 100 cm^{-1} for **1g** and **1d**, respectively, were found to depend strongly on the substitution on the N donor atom. To determine the origin of these discrepancies in s values, we studied variations of a^3 and of $\Delta\mu$ in **1a**−**i**. The volume a^3 of the molecular cavity was assumed to be proportional to the molecular volume $V' = V/Z$ with V being the elementary cell volume and Z the number of molecules in each cell; values of V', assessed from crystallographic data reported below. They are reported In Table 1. The factor $\sqrt{sV'}$, related to $\Delta\mu$ following eq 2, was found to present nearly constant values for **1a**−**i**, with slightly higher values for **1c** and **1d**.

This trend can be easily interpreted for **1d**, for which a higher value of $\Delta\mu$ can be ascribed to an increase of the ICT due to either a higher planarity of the molecule in solution or a higher donor efficiency of the diphenyl amino group with respect to other substituents of this family (all dialkyl amino). The fact that molecules **1a**−**c** present a red-shifted absorption, with absorption maxima at 514, 509, and 507 nm, respectively, against 491 nm for **1d**, allows us to conclude there is an ICT enhancement in the excited state and not in the ground state. In good agreement with this assumption, the largest bathochromic shift of the luminescence band is found for **1d** with an emission centered at 692 nm, and then with the highest stokes shift values of 5916 cm^{-1} for this family (Table 1). Quantum yields of fluorescence (Φ_f) were measured in dilute dichloromethane and are reported in Table 1. A significant dependence of the fluorescence quantum yield with both substituents and solvent was observed. With Φ_f of 20%, the fluorophore **1d** with a *N*,*N*-diphenylamino donor group is the most emissive molecule of the series. This value is the same as reported previously by others (21% in the same solvent).[14a] The *N*,*N*-dialkyl substituted compounds (**1a**, **1b**, and **1c**) showed similar fluorescence quantum yield, but weaker than the diphenyl analogue and higher than those of species having heteroatoms on the β position of the ethylene group borne by the N donor atom (molecules **1e**−**i**). Such a decrease in quantum yield can temptingly be attributed to a decrease of the donating ability of the nitrogen atom and thus a decrease of the charge transfer and/or an electron transfer quenching mechanism from the electronegative heteroatom. Such a trend is in good agreement with the blue shift of absorption and emission bands for these molecules with respect to those of molecules **1a**−**c**. Quantum yields in other solvents were not measured, but for all compounds the intensity of fluorescence increases with the solvent polarity (cyclohexane/toluene < ethylacetate < dichloromethane ≪ acetonitrile/methanol < DMSO).

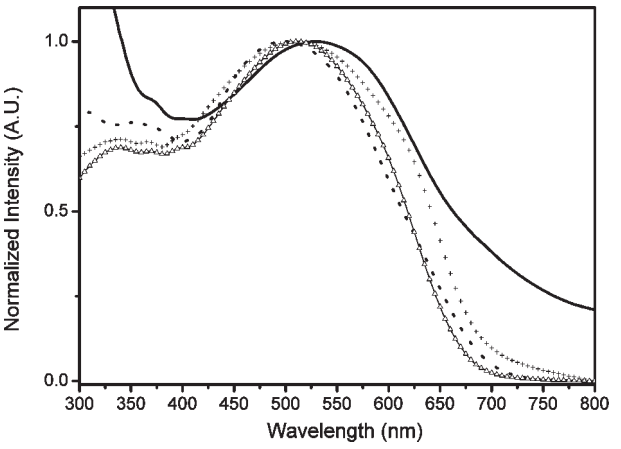

Figure 3. Absorption spectra **1c** (—), **1d** (····), **1h** (+), and **1i** (Δ), crystals grounded in magnesium oxide.

Properties of Crystals. Crystals suitable for X-ray diffraction were grown by slow diffusion of n-heptane in concentrated solution in diethylether (for compounds **1a**, **1e**, **1i**), of cyclohexane in concentrated solution in dichloromethane (for compounds **1c**, **1f**, **1g**, **1h**), by slow diffusion of toluene in a concentrated acetonitrile solution (for **1d**) and by slow diffusion of vapor of pentane to a concentrated solution in toluene for **1b**. Figure 3 shows absorption spectra of crystals of **1c**, **1d**, **1f** and **1i** grounded in anhydrous magnesium oxide (data for other compounds are given in Figure S13 in the Supporting Information). All spectra are considerably broadened and red-shifted compared to the solution with $\Delta\lambda$ between 32 and 17 nm for **1g** and **1b**, respectively (Table 2). A significant lower value was observed for **1d** (9 nm). However, these bands are likely the overlap of at least two bands as a shoulder above 600 nm can clearly be seen for **1f** (Figure 3) and other compounds in Figure S13 in Supporting Information. This suggests the existence of excitons in the solid state and the fluorescence data seem to confirm this observation.

Figure 4 shows the emission of crystals of **1i** under illumination of a handled UV lamp at 365 nm, which is far from their excitation maximum, as shown by data below. Excitation and emission spectra were recorded on crystals using the front-face configuration of the spectrofluorimeter. They are shown in Figure 5 for **1c**, **1d**, **1f**, and **1i** and Figures S14−S15 in Supporting Information for all other compounds. Emission spectra were recorded first with an excitation wavelength at 515 nm close to the absorption maximum found in magnesium oxide. Only one structureless emission peak was observed whatever the compound, with a large red shift compared to emission observed in solution with $\Delta\lambda$ values from 168 to 116 nm for **1h** and **1b** respectively (Table 2); lower values of 50 and 80 nm were obtained for **1d** and **1i** respectively.

Table 2. Spectroscopic Properties in the Solid-State[a]

	λ_{abs}^{ss} [b] (nm)	λ_{exc}^{ss} [c] (nm)	λ_{em}^{ss} [d] (nm)	$\Delta\tilde{\nu}^{ss}$ [e] (cm^{-1})	$\Delta\tilde{\nu}^{ss}$ [f] (cm^{-1})
1a	545 (31)	600/672	781 (123)	5544	2077
1b	526 (17)	broad	773 (116)	6074	
1c	531 (23)	531/633	783 (126)	6061	3026
1d	498 (9)	broad	740 (50)	6567	
1e	512 (20)	520/646	775 (132)	6628	2576
1f	509 (32)	551/654	750 (118)	6313	1957
1g	509 (19)	527/644	774 (131)	6726	2608
1h	495 (22)	514/624	791 (168)	7560	3383
1i	512 (28)	495/610	716 (80)	5564	2426

[a] Maxima of absorption λ_{abs}^{ss} in MgO (difference with the dichloromethane solution), of excitation λ_{exc}^{ss} in crystal, of steady-state fluorescence emission λ_{em}^{ss} in crystal (difference with the dichloromethane solution) and Stokes shift $\Delta\tilde{\nu}^{ss}$. [b] Grounded crystal in magnesium oxide. [c] Deconvolution of two peaks. [d] λ_{exc} = 515 nm, $\lambda_{exc} = \lambda_{exc}^{ss}$. [e] Calculated from the absorption spectra. [f] Calculated from the excitation spectra.

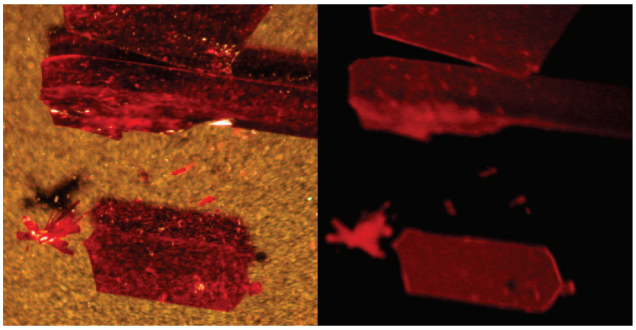

Figure 4. Photograph of crystals of **1i** (left) and the same under illumination of handled UV lamp at 365 nm (right).

Excitation spectra were recorded with an emission wavelength set up to the maximum of emission. The excitation spectra are the overlap of at least two peaks. Good deconvolution with two peaks can be achieved, giving a broad peak at lower wavelength and a sharp peak with a maximum above 600 nm for each compound. The relative intensities of the two peaks vary from one compound to another. Hence, for the *N*,*N*-dialkyl compounds **1a**, **1b**, **1c**, and especially the diphenyl **1d**, the excitation spectra mainly display a broad peak that globally matches the absorption spectra. For **1a**, **1b**, **1c**, a maximum at higher wavelength can nevertheless be seen, whereas a shoulder is hardly present in the spectrum of **1d**. For the other compounds, the sharp peak at higher wavelength is predominant. It is important to note that the emission remained unchanged when varying the excitation wavelength, indicating that both bands correspond to the same emitting center.

For all compounds, the emission maxima are above 700 nm and the emission bands are broad and cut by the detection limit (850 nm) of the Hamamatsu R928 photomuliplier. Determination of quantum yield is therefore hampered. As a consequence, only the intensity at the maximum emission can be compared. The less emissive compounds are **1a**, **1b**, **1c**, then the diphenyl **1d** and the compounds with chlorine atoms **1g** and **1h**. Compounds **1e** and **1f** present a rather intense emission in comparison, whereas the diacetoxyethyl compound **1i** is by far the most emissive compound, with intensity at the maximum

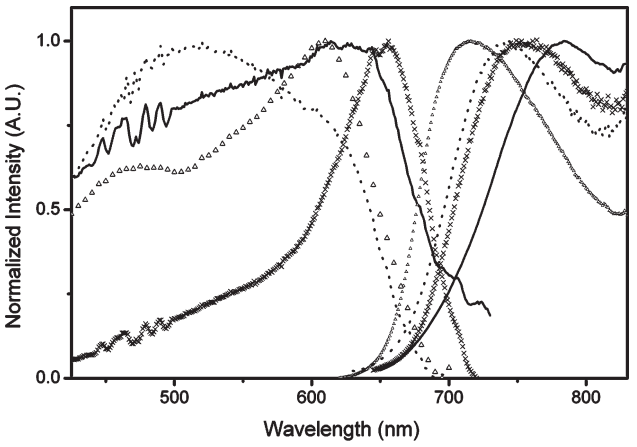

Figure 5. Excitation and emission spectra of **1c** (—), **1d** (····), **1f** (×), and **1i** (Δ) in the solid state (crystals).

25 times more intense than **1e** and almost 170 times more than **1c** for the same instrument configuration.

To interpret the origin of the emission in crystals and of the nature of this two peaks, we selected the case of **1d** and **1f,** as those two compounds present dramatically different excitation and emission characteristics. The absorption/excitation and emission maxima of **1d** are less red-shifted with respect to those observed in solution ($\Delta\lambda$ of 9 and 50 nm for absorption and emission respectively and a Stokes shift of 5940 cm^{-1} in crystals, comparable to 5916 cm^{-1} in solution) than are those of other compounds. It is worth noting that the emission of **1d** in crystal (740 nm) is now the one occurring at the shortest wavelength, while it was that at the longest wavelength in solution (692 nm). The small red-shift may be due to a higher planarity of the molecule in solid state compared to the solution or more probably to aggregation and the presence of excitons presenting parallel transition dipole, as is suggested by the broadening and splitting of the band (with a shoulder at 621 nm in both the absorption and excitation spectra) and confirmed by the weaker emission observed with this compound. Results obtained for **1f** are very different. This molecule presents an emission centered at 750 nm (with a net red-shift of $\Delta\lambda$ = 118 nm compared to the solution in dichloromethane and 64 nm compared to the fluorescence in the most polar solvent), which is mainly excited in a sharp band at 653 nm and weakly at 555 nm. In this case, the Stokes shift is significantly shorter (1957 cm^{-1}) than in the case of **1d** (6094 cm^{-1}).This looks like a pure aggregate case with in-line transition dipoles,[19] as also suggested by the sharp excitation spectrum. Other molecules (**1e**, **1g**, **1h**) display very similar excitation spectra (Figure 5 and Figure S15 in the Supporting Information) with a main sharp peak at longest wavelengths ($\Delta\lambda$ = 168 nm for **1h** compared to dichloromethane solution and still 115 nm

(19) Kasha, M.; Rawls, H. R.; El-Bayoumi, A. M. *Pure Appl. Chem.* **1965**, *11*(3), 371.
(20) Boens, N.; Qin, W.; Basarić, N.; Hofkens, J.; Ameloot, M.; Pouget, J.; Lefèvre, J.-P.; Valeur, B.; Gratton, E.; vandeVen, M.; Silva, N. D. J.; Engelborghs, Y.; Willaert, K.; Sillen, A.; Visser, A. J. W. G.; van Hoek, A.; Lakowicz, J. R.; Malak, H.; Gryczynski, I.; Szabo, A. G.; Krajcarski, D. T.; Tamai, N.; Miura, A. *Anal. Chem.* **2007**, *79*(5), 2137.

Table 3. Crystal Data and Structure Refinement Parameters

	1a	1b	1c	1d	1e	1f	1g	1h	1i
formula	$C_{23}H_{27}N_3$	$C_{58}H_{62}N_6$	$C_{33}H_{39}N_3$	$C_{33}H_{30}N_4$	$C_{23}H_{26}N_6$	$C_{23}H_{25}N_9$	$C_{23}H_{26}ClN_3$	$C_{23}H_{25}Cl_2N_3$	$C_{27}H_{31}N_3O_4$
cryst syst	monoclinic	monoclinic	monoclinic	monoclinic	triclinic	monoclinic	orthorhombic	triclinic	monoclinic
space group	$P2_1/c$ (No. 14)	$P2_1$ (No. 4)	$P2_1/c$ (No. 14)	$P2_1/c$ (No. 14)	P-1 (No. 2)	$P2_1/c$ (No. 14)	$Pbca$ (No. 61)	P-1 (No. 2)	$P2_1/c$ (No. 14)
a (Å)	8.358 (5)	8.552 (5)	13.408(5)	9.173 (5)	7.671 (5)	10.920 (5)	15.7228 (5)	9.244 (5)	17.727 (5)
b (Å)	17.836 (5)	7.519 (5)	24.237(5)	18.158 (5)	8.752 (5)	14.000 (5)	11.5429 (5)	10.877 (5)	17.596 (5)
c (Å)	13.691 (5)	38.551 (5)	12.104(5)	16.718 (5)	16.741 (5)	15.753 (5)	23.123 (5)	13.234 (5)	8.291 (5)
α (deg)	90.0	90.0	90.0	90.0	96.328	90.0	90.0	70.273 (5)	90.0
β (deg)	96.544 (5)	91.896 (5)	94.719(5)	97.576 (5)	93.545	106.26 (5)	90.0	70.515 (5)	91.537 (5)
γ (deg)	90.0	90.0	90.0	90.0	95.462	90.0	90.0	65.327 (5)	90.0
V (Å^3)	2057 (2)	2478 (2)	3920 (2)	2760 (2)	1124 (2)	2312 (4)	4196 (1)	1109 (1)	2585 (2)
Z	4	2	4	4	2	4	8	2	4

Table 4. Selected Bond Distances (Å) and Torsion Angles (def) for All Compounds

	C_1-C_2	$C_2=C_3$	C_3-C_4	$C_4=C_5$	C_5-C_6	$C_6=C_7$	Δ	θ_1	θ_2	θ_3
1a	1.444(8)	1.33(1)	1.449(8)	1.36(1)	1.418(9)	1.36(1)	0.038	179.2(6)	178.7(7)	−177.0(7)
1b	1.439(8)	1.345(8)	1.431(8)	1.346(8)	1.425(8)	1.350(8)	0.026	−176.1(6)	−178.3(6)	176.0(6)
	1.431(8)	1.332(8)	1.437(8)	1.366(8)	1.416(8)	1.358(8)	0.073	−175.4(6)	−177.8(6)	−178.5(6)
1c	1.48(2)	1.29(2)	1.44(2)	1.34(2)	1.38(2)	1.44(3)	0.072	176(2)	−179(2)	−172(2)
1d	1.458(3)	1.346(4)	1.445(3)	1.359(4)	1.418(3)	1.366(4)	0.099	−177.5(2)	179.3(2)	179.2(2)
1e	1.441(5)	1.345(5)	1.437(5)	1.354(6)	1.425(6)	1.351(7)	0.029	−179.0(4)	178.4(4)	179.8(4)
1f	1.453(5)	1.331(6)	1.450(4)	1.341(6)	1.426(4)	1.357(6)	0.091	−176.6(4)	−177.1(4)	−172.0(4)
1g	1.441(6)	1.346(6)	1.435(6)	1.348(6)	1.426(6)	1.368(6)	0.035	179.2(4)	179.6(5)	176.8(4)
1h	1.447(4)	1.338(3)	1.437(4)	1.358(3)	1.422(4)	1.361(3)	0.029	−176.4(3)	−178.1(3)	176.5(3)
1i	1.462(9)	1.35(1)	1.43(1)	1.36(1)	1.41(1)	1.38(1)	0.161	−160.3(7)	−179.1(7)	−179.9(7)

compared to the most polar solvent) corresponding to aggregates (with shorter Stokes shift from 1957 to 3380 cm^{-1}) and a more or less intense band in the blue range corresponding to the planar monomer. As already mentioned and shown by the broad excitation spectra, **1a**, **1b**, and **1c** are intermediate cases, even if the emission arises from aggregates and are closed to that of **1f** (from 773 to 783 nm with $\Delta\lambda$ from 115 to 126 nm as compared to dichloromethane solution). The crystal of **1i** presents a similar excitation spectrum than other previous molecules, but exhibits an emission at 716 nm only with a $\Delta\lambda$ value of 80 nm.

These data allow attributing the crystal emission of these molecules to aggregates. To gain further insight into the solid-state emissive behavior of theses fluorophores, we have also studied the details of the molecular packing in their single crystal, which could allow identifying the nature of aggregates. Molecular packing modes are generally dictated by the nature of the interactions (strong and weak) between molecules that decide the bulk arrangement of the molecules. It is important to note that the crystals for X-ray diffraction were chosen among those used for the fluorescence studies.

Crystal Structure. Crystallographic data and basic structural parameters are given in Table 3. Selected distances and dihedral angles are compiled in Table 4. The atom numbering scheme common to all structures with the angles and distance definition are given in Figure 6. The asymmetric units are composed of one molecule except for **1b**, where two packed molecules are present. The molecular structures are very similar for all compounds with only the all *trans* rotamer present. The conjugated system is almost planar with 27 atoms forming a mean plane. The puckering amplitude to the mean plane for the 27 atoms Δ does not exceed 0.099 Å, except for the most distorted structure **1i** (0.161 Å). The dihedral angles measured between the phenyl ring and the

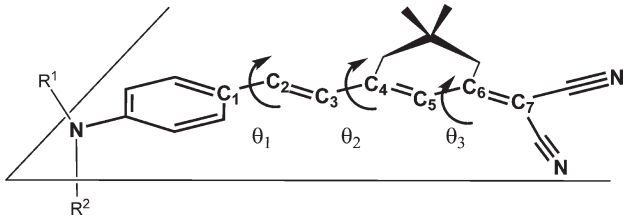

Figure 6. Molecular structure, atom numbering (different than the cif file), and angles. The 27 atoms forming the mean plane are drawn in bold.

$C_2=C_3$ double bond (θ_1) ranged from 0.8° for **1a** and **1g** to 19.7° for the most distorted structure (**1d**). The dihedral angles measured between the two central double bonds $C_2=C_3$ and $C_4=C_5$ (θ_2) and between the $C_4=C_5$ and $C_6=C_7$ double bonds on the acceptor part (θ_3) ranged between 0.4 and 2.9° and 0.1 and 8°, respectively, indicative of a full conjugation between the donor and the acceptor end. Substituent groups on the N-donor atom are arranged on both sides of the molecular mean plane, whereas the dimethylmethylene group of the isophorone ring lays 0.7 Å above the plane.

The diethylamino compound **1a**, the racemic hexyl(1-phenylethyl)amino **1c**, the diphenylamino **1d**, the di-(2-ethyl(1-phenylethyl)amino)amino **1f** and the di(acetoxyethyl)amino compounds **1i** crystallized in the monoclinic $P2_1/c$ group with an elemental cell containing four molecules. The chiral ethyl-(1-phenylethyl)amino compound **1b** crystallized in the monoclinic $P2_1$ group with a unit cell containing two sets of two molecules. The (2-ethyl(1-phenylethyl)amino)ethylamino **1c** and the di-(2-chloroethyl)amino **1h** crystallized in the triclinic *P-1* group with two molecules in the unit cell, whereas the (2-chloroethyl)ethylamino compound **1g** crystallized in the orthorhombic *Pbca* group with eight molecules in the unit cell. Partial crystal packing diagrams are shown in Figure 7 to Figure 15.

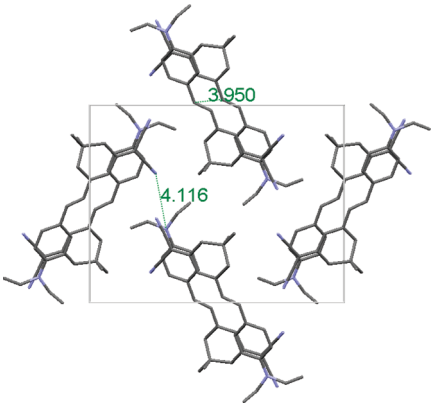

Figure 7. Packing diagram of the cell of **1a**, viewed down the crystallographic *a* axis.

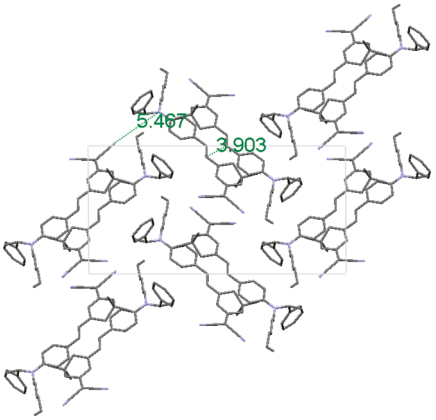

Figure 8. Packing diagram of the cell of **1c**, viewed down the crystallographic *a* axis.

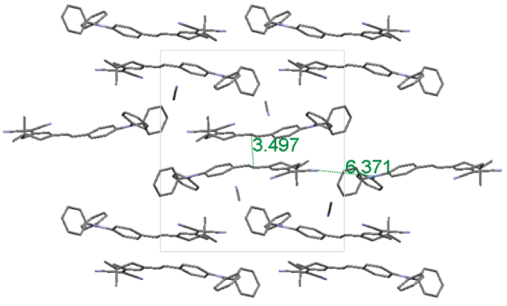

Figure 9. Packing diagram of the cell of **1d**, viewed down the crystallographic *a* axis.

Face-to-face H-type dimers can be observed in the crystal packing of the diethylamino **1a**, of the chiral ethyl(1-phenylethyl)amino compound **1b**, in which they constitute the two molecules of the asymmetric unit, of the racemic hexyl(1-phenylethyl)amino **1c** and of the diphenylamino compound **1d**. Significant differences can nevertheless be observed. The two conjugated systems of the two face-to-face dipoles do not always closely packed and are often slipped away. The dipole−dipole distance ranges from 3.49 Å for **1d** to 3.95 Å for **1a** (Figures 7−9), but is longer for **1b** (4.232 Å). In that case, the molecular planes are not exactly coplanar but slightly tilted by 3.96° (Figure 10). For all compounds, the

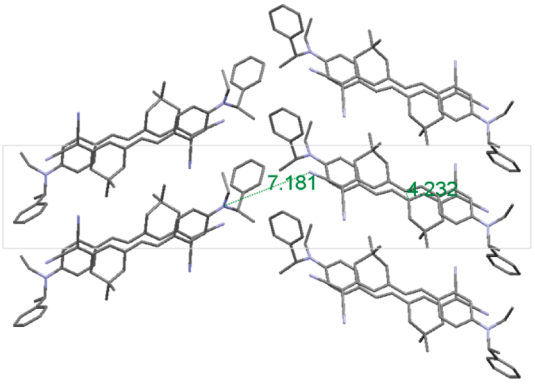

Figure 10. Packing diagram of the cell of **1b**, viewed down the crystallographic *a* axis.

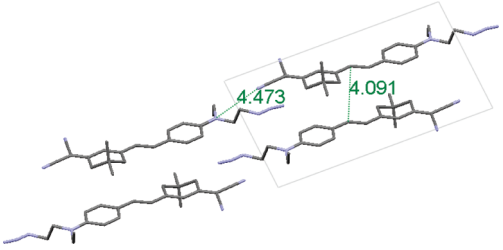

Figure 11. Crystal packing of **1e** viewed down the crystallographic *a* axis.

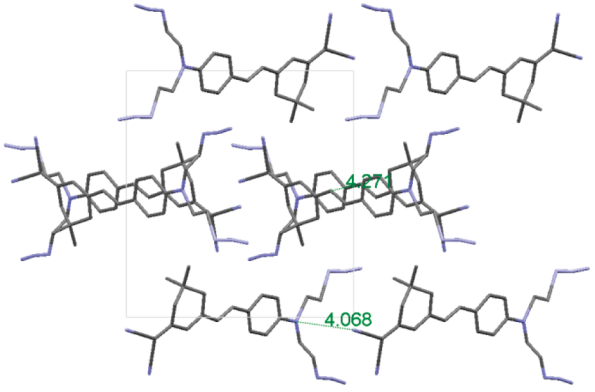

Figure 12. Crystal packing of **1f** viewed down the crystallographic *a* axis.

centroids of the two interacting dipoles do not face each-other but are slipped away, characteristic of coplanar inclined transition dipoles.[19] This corroborated the large excitation spectra and the weaker emission observed for all these compounds.

The crystal packing of (2-azidoethyl)ethylamino **1e**, of di-(2-azidoethyl)amino (2-chloroethyl)ethylamino **1f**, and of di-(2-chlororoethyl)ethylamino **1h** (Figures 11−13) are all composed of antiparallel chain of dipoles. In a chain, all dipoles are oriented in the same direction, whereas two neighboring chains have opposite direction. The distances between two head-to-tail dipoles from two antiparallel chains (from 3.86 Å for **1e** and **1h** to 3.97 for **1f** for the closest distance, although the distances between the molecular main planes are slightly longer) are very similar to the distances between the acceptor-end of one dipole and the donor-end of the following dipole in a chain (from 4.00 for **1f**

to 4.47 for **1e**). A herringbone pattern with accentuated vertices (78.5°) and short interplane distances (3.654 Å) best describes the crystal packing for the (2-chloroethyl)ethylamino compound **1g** (Figure 14). In that example, no H-aggregates are seen. Head-to-tail dipoles are slipped away with respect to each other and do not closely pack. Actually the closest dipole−dipole distance is 3.65 Å between the acceptor end-group and the N donor atom of the following dipole constituting the vertex. The presence of long chains of molecules for **1e**, **1f**, **1h**, and **1g** is in agreement with the crystal fluorescence observed and allows attributing the sharp excitation peak and the fluorescence emission to J-type aggregates for these compounds.

Finally, for the di(acetoxyethyl)amino **1i**, no stacking and no specific aggregate could be observed (Figure 15). It is worth noting that **1i** is also the most fluorescent molecule in the solid state and the less red-shifted among the series.

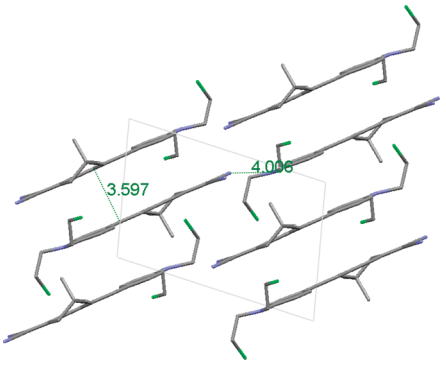

Figure 13. Crystal packing of **1h** viewed down the crystallographic *b* axis.

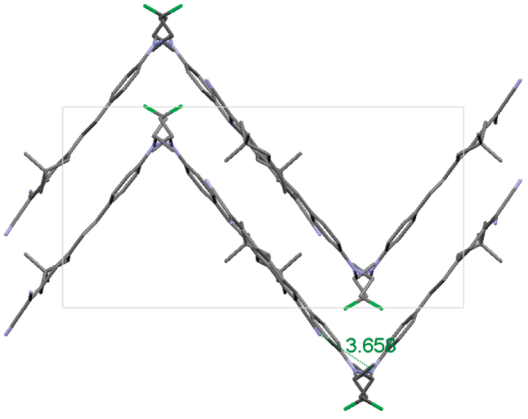

Figure 14. Packing diagram of the cell of **1g** viewed down the crystallographic *a* axis.

Conclusion

In this work, we synthesized and studied the crystal structure, the solution, as well as the solid-state fluorescent properties of nine push−pull dipolar fluorophores based on the dicyanoisophorone acceptor group and differing only by the substituent groups borne by the N donor atom. This study showed a significant influence of the substituent groups not only on the fluorescence properties in solution but also on the crystal packing and hence on the solid-state fluorescence properties that were attributed to likely arise from aggregates observed in the crystal structure. By varying the substituent groups, emission in the near-infrared ranging from 715 to 790 nm can be obtained, whereas sharp excitation in the red (from 610 to 670 nm) is achieved. This is of particular interest for the development of biochips or the use of nanocrystals for bioimaging as the emission is in the biological transparency window. Highly conjugated dipolar molecules are likely to possess good two-photon absorbing properties and two-photon excitation in the range 900−950 nm can be envisaged to bring both the excitation and the emission in the transparency window. In that perspective, the most interesting compound, which showed the highest crystal fluorescence (Figure 4), is **1i** bearing two acetoxyethyl groups. Developments in that way are currently being undertaken in our group.

Experimental Section

General. ^{1}H and ^{13}C NMR spectra were recorded at room temperature on Bruker AC 200 spectrometer. ^{13}C NMR spectra were recorded with complete proton decoupling. Chemical shifts are reported in ppm from tetramethylsilane with the solvent resonance as internal standard. For proton, data are reported as follows: chemical shift, multiplicity (*s* = singlet, *d* = doublet, *t* = triplet, *q* = quartet, *m* = multiplet, *b* = broad), coupling constants in Hz. Microanalyses and high-resolution mass spectra were performed at the Service Central d'Analyze du CNRS (Vernaison, France). UV/vis absorption measurements were recorded on a JASCO V550 spectrometer for the solution. Crystals were grounded with anhydrous magnesium oxide and the absorption recorded using an integration sphere. Fluorescence spectra were measured using a Horiba-Jobin Yvon Fluorolog-3 spectrofluorimeter, equipped with a red-sensitive Hamamatsu R928 photomuliplier tube and the spectra recorded in front-face configuration. The crystals were mounted on a solid-state holder. Spectra were reference corrected for both the excitation source light intensity variation (lamp and grating) and the emission spectral response (detector and grating). All

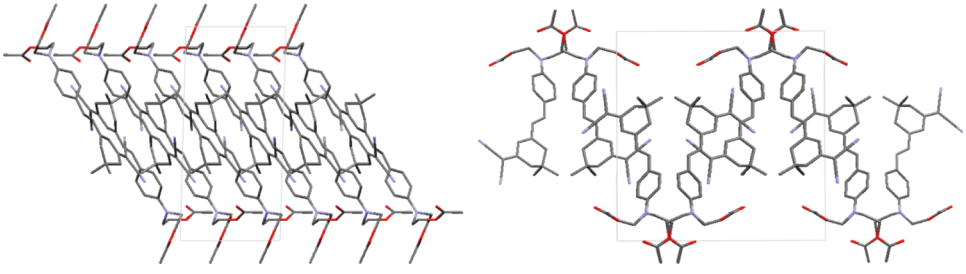

Figure 15. Packing diagram of the cell of **1i**, viewed down the crystallographic *b* axis (left) and down the *c* axis (right).

solvents were of spectrophotometric grade. Rubrene was purchased from Acros.

All air- or moisture-sensitive reactions were carried out in flame-dried glassware under Ar atmosphere. Anhydrous DMF was purchased from Acros. Thin-layer chromatography (tlc) was performed with Merck 60F254 precoated silica gel plates. Column chromatography was carried out using Merck silica gel 60 (35−70 μm).

*General Protocol A. Synthesis of **3a**−**i***. Under argon, aniline derivative **2a**−**i** (1 equiv.) was dissolved in dry DMF (10 equiv) and the solution was cooled to 0 °C with an ice bath. $POCl_3$ (2 equiv.) was slowly added. The mixture was stirred for a given time (see detailed for every product) at 40 °C (unless otherwise stated). After cooling to room temperature, the green solution was poured into ice water and carefully neutralized with solid K_2CO_3. The aqueous layer was extracted three times with CH_2Cl_2 (3 × 10 mL) and the combined organic phases were washed three times with water (3 × 10 mL) and once with brine (10 mL), dried over sodium sulfate, and concentrated under reduced pressure to afford pure compounds.

*General Protocol B. Synthesis of **1a**−**i***. Under argon, compound **3a**−**i** (1 equiv.) and 2-(3,5,5-trimethylcyclohex-2-enylidene)malononitrile **4** (1 equiv.) were dissolved in dry acetonitrile (100 mL for 14 mmol). Piperidine (0.01 equiv) was added and the solution was stirred at 40 °C for 8 h. The red solution was concentrated and the product purified by crystallization or column chromatography.

2-(3,5,5-Trimethylcyclohex-2-enylidene)malononitrile (***4***). To a solution of isophorone (2.1 mL, 13.8 mmol, 1 equiv.) and malononitrile (912 mg, 13.8 mmol, 1 equiv.) in dry ethanol (150 mL) was added piperidine (13 mL, 0.14 mmol, 0.01 equiv.). The solution was stirred at 60 °C for 8 h. After cooling to room temperature, the black solution was slowly poured into water (200 mL) and the precipitated black solid was filtered. Recrystallization from heptane afforded a brown solid. Yield: 2.3 g (90%). ^{1}H NMR ($CDCl_3$): δ 6.61 (s, 1H), 2.51 (s, 2H), 2.17 (s, 2H), 2.02 (s, 2H), 1 (s, 6H, $-CH_3$). ^{13}C NMR ($CDCl_3$): δ(ppm) 170.5, 160, 120.5, 45.6, 42.6, 32.4, 27.8, 25.3. IR (KCl, cm^{-1}) 2219 (ν_{CN}). Anal. Calcd for $C_{12}H_{14}N_2$: C, 77.38; H, 7.58; N, 15.04. Found: C, 77.73; H, 7.53; N, 15.45. m.p.: 73−75 °C.

(*R*)-*N*-(*1-Phenylethyl*)*aniline* (***5***). To a solution of (*R*)-α-methylbenzylamine (956 μL, 7.5 mmol) and iodobenzene (666 μL, 5 mmol) in anhydrous DMSO was added in order CuI (95 mg, 0.5 mmol), L-proline (115 mg, 1 mmol), and K_2CO_3 (1.38 g, 10 mmol.) The mixture was heated at 80 °C for 20 h. After cooling to room temperature, the mixture was partitioned between dichloromethane (30 mL) and water (10 mL). The organic layer was dried with Na_2SO_4, filtered and evaporated, and the crude purified by chromatography on silica eluting with chloroform. Yield: 820 mg (83%), colorless oil. Racemic (±)-N-(1-phenylethyl)aniline **6** was obtained starting from (±)-α-methylbenzylamine. ^{1}H NMR ($CDCl_3$): δ 7.38−7.20 (m, 5H), 7.08 (dd, 2H, J = 7.5 Hz, J = 8.0 Hz), 6.63 (t, 1H, J = 7.25 Hz), 6.50 (d, 2H, J = 7.7 Hz), 4.47 (q, 1H, J = 6.7 Hz, −CH−), 4.00 (b s, 1H, -NH-), 1.50 (d, 3H, J = 6.7 Hz, $-CH_3$). ^{13}C NMR $CDCl_3$): δ 147.3 (C^{IV}), 145.2 (C^{IV}), 129.0, 128.6, 126.8, 125.8, 119.5, 117.2, 113.3, 53.4, 25.0.

(*R*)-*N-Ethyl-N*-(*1-phenylethyl*)*aniline* (***3b***). To a solution of **5** (800 mg, 4 mmol) in anhydrous DMF (3 mL) was added iodoethane (1.6 mL, 20 mmol) and Na_2CO_3 (1.06 g, 10 mmol). The mixture was heated at 65 °C for 3 days, and then cooled to room temperature and partitioned between water (10 mL) and dichloromethane (30 mL). The organic layer was dried with Na_2SO_4, filtered and evaporated, and the crude purified by chromatography on silica eluting with chloroform. Yield: 720 mg (80%), colorless oil. ^{1}H NMR ($CDCl_3$): δ 7.36−7.12 (m, 7H), 6.84 (d, 2H, J = 8.16 Hz), 6.74 (t, 1H, J = 7.2 Hz), 5.09 (q, 1H, J = 6.9 Hz, −CH−), 3.25 (t, 2H, J = 7.0 Hz, $-NCH_2-$), 1.61 (d, 3H, J = 6.9 Hz, $-CHC\underline{H}_3$), 1.10 (t, 3H, 3H, J = 7.0 Hz, $-CH_2C\underline{H}_3$). ^{13}C NMR ($CDCl_3$): δ 148.0 (C^{IV}), 143.0 (C^{IV}), 129.1, 128.3, 127.0, 126.7, 116.5, 113.8, 56.7 (−CH−), 40.2 ($-CH_2-$), 17.6 ($-CH_2\underline{C}H_3$), 14.2 ($-CH\underline{C}H_3$).

(±)-*N-Hexyl-N*-(*1-phenylethyl*)*aniline* (***3c***). To a solution of **6** (750 mg, 3.8 mmol) in anhydrous DMF (3 mL) was added n-hexylbromide (2.1 mL, 15.2 mmol), NaI (2.25 g, 15.2 mmol), and Na_2CO_3 (750 mg, 7.5 mmol.) The mixture was heated at 95 °C for 20 h, and then cooled to room temperature and partitioned between water (10 mL) and dichloromethane (30 mL). The organic layer was dried with Na_2SO_4, filtered and evaporated, and the crude purified by chromatography on silica eluting with chloroform. Yield: 800 mg (75%), colorless oil. ^{1}H NMR ($CDCl_3$): δ 7.30−7.18 (m, 7H), 6.81−6.67 (m, 3H), 5.03 (q, 1H, J = 6.7 Hz, −CH−), 3.08 (m, 2H), 1.59−1.48 (m, 3H +2H), 1.20 (m, 6H), 0.84 (m, 3H). ^{13}C NMR ($CDCl_3$): δ 148.8 (C^{IV}), 142.0 (C^{IV}), 129.1, 128.3, 127.1, 126.7, 116.5, 113.9, 57.0 (−CH−), 46.3, 31.5, 28.4, 26.8, 22.6, 17.5, 14.0

(*R*)-*4*-(*Ethyl*(*1-phenylethyl*)*amino*)*benzaldehyde* (***2b***). **2b** was obtained according to general protocol A from **3b** (112 mg, 0.5 mmol.), $POCl_3$ (55 μL, 0.6 mmol.) and DMF (5 mL). Yield: 150 mg (100%). Used immediately without further purification.

(±)-*4*-(*Hexyl*(*1-phenylethyl*)*amino*)*benzaldehyde* (***2c***). **2c** was obtained according to general protocol A from **3c** (112 mg, 0.5 mmol), $POCl_3$ (55 μL, 0.6 mmol), and DMF (5 mL). Yield: 150 mg (100%), used immediately without further purification.

4-(*Diphenylamino*)*benzaldehyde* (***2d***). Under argon, $POCl_3$-(2.8 mL, 30 mmol, 1.5 equiv.) was slowly added to dry DMF(10 mL, 0.13 mol, 6.5 equiv.) at 0 °C. After 20 min triphenylamine(5 g, 20 mmol, 1 equiv.) was added. The mixture was stirred at room temperature during 10 h. The green solution was poured into ice water and carefully neutralized with solid K_2CO_3. The aqueous layer was extracted three times with CH_2Cl_2(3 × 20 mL) and the combined organic phases were washed three times with water(3 × 20 mL), once with brine(20 mL) and dried over sodium sulfate. The solvent was removed and purification by column chromatography on silica (CH_2Cl_2) afforded a pale green solid (4.7 g, 86%). ^{1}H NMR (Acetone-d6): δ(ppm) 9.83 (s, 1H), 7.73 (d, J = 10 Hz, 2H), 7.31 (m, 10H), 6.97 (d, J = 10 Hz, 2H). ^{13}C NMR (Acetone-d6): δ(ppm) 147.2, 190.1, 131.9, 130.7, 127.3, 126.1, 119.8. IR (KCl, cm^{-1}) 3448, 1689. Anal. Calcd for $C_{19}H_{15}NO$: C, 83.49; H, 5.53; N, 5.12. Found: C, 83.66; H, 5.59; N, 5.49. HR-MS (ES^+): $[M + H]^+$ 274.1240 (calcd 274.1232). m.p.-(heptane): 133 °C.

N-(*2-Azidoethyl*)-*N-ethylaniline* (***3e***). *N*-Ethyl-*N*-hydroxyethylaniline (4.9 mL, 30.2 mmol, 1 equiv.) was dissolved in Et_2O (25 0 mL) and the solution was cooled to 0 °C with an ice bath. Et_3N (4.6 mL, 33.3 mmol, 1.1 equiv.) was added slowly, followed by methanesulfonyl chloride (2.6 mL, 33.3 mmol, 1.1 equiv.). After stirring at room temperature for 1 h, the white mixture was filtered-off and the filtrate concentrated. The green oil was dissolved DMSO (100 mL) and sodium azide (3.9 g, 60.5 mmol, 2 equiv) was added. The mixture was stirred at 80 °C for 3 h, cooled to room temperature and the suspension was diluted with water (100 mL). The aqueous layer was extracted three times with Et_2O (3 × 100 mL) and the combined organic phases were washed with brine (100 mL), dried over sodium sulfate and concentrated under reduced pressure to afford a pale yellow oil. Yield: 5.52 g (96%). ^{1}H NMR (CD_2Cl_2): δ (ppm) 7.27 (t, J = 7.1 Hz, 2H), 6.76 (m, 3H), 3.49

(m, 6H), 1.22 (t, J = 7 Hz, 3H). ^{13}C NMR (CD_2Cl_2): δ (ppm) 146.1, 128, 115.2, 111, 48.3, 47.8, 44.1, 10.7. IR (KCl, cm^{-1}) 2103 (νN_3). Anal. Calcd for $C_{10}H_{14}N_4$: C, 63.13; H, 7.42; N, 29.45. Found: C, 63.02; H, 7.47; N, 28.14. HR-MS (ES$^+$): [M + H]$^+$ 190.1293 (calcd. 190.1297).

N,N-Bis(2-azidoethyl)aniline (***3f***). **3f** was synthesized accordingly starting from *N*-Phenyldiethanolamine (5.5 g, 30.2 mmol, 1 equiv) Et_3N (4.6 mL, 33.3 mmol, 1.1 equiv) and methanesulfonyl chloride (5.2 mL, 66.6 mmol, 2.2 equiv) in Et_2O (250 mL), then sodium azide (7.8 g, 121 mmol, 4 equiv) in DMSO (100 mL). (6.6 g, 94%). ^{1}H NMR (Acetone-d6): δ(ppm) 7.22 (t, J = 8 Hz, 2H), 6.83 (d, J = 8 Hz, 2H), 6.68 (t, J = 8 Hz, 1H), 3.59 (m, 8H). ^{13}C NMR (Acetone-d6): δ(ppm) 147.7, 130.16, 118, 113.5, 51, 49.5. IR (KCl, cm^{-1}) 2100 (νN_3). Anal. Calcd for $C_{10}H_{13}N_7$: C, 51.94; H, 5.67; N, 42.40. Found: C, 51.34; H, 5.65; N, 42.39. HR-MS (ES$^+$): [M + H]$^+$ 232.1304 (calcd 232.1311).

4-((2-Azidoethyl)(ethyl)amino)benzaldehyde (***2e***). **2e** was obtained according to general protocol A from **3e** (5 g, 26.3 mmol.), $POCl_3$ (4.9 mL, 52.6 mmol.) and DMF (20 mL). Yield: 9 g (85%). ^{1}H NMR ($C_2D_2Cl_4$): δ(ppm) 10.4 (s, 1H), 8.42 (d, J = 8.8 Hz, 2H), 7.43 (d, J = 8.8 Hz, 2H), 4.2 (m, 6H), 1.9 (t, J = 6.9 Hz, 3H). ^{13}C NMR ($C_2D_2Cl_4$): δ(ppm) 189.8, 151.8, 132, 125.1, 110.9, 49, 48.6, 45.4, 11.9. IR (KCl, cm^{-1}) 2102 (νN_3), 1666. HR-MS (ES$^+$): [M + H]$^+$ 219.1241 (calcd 219.1246).

4-(Bis(2-azidoethyl)amino)benzaldehyde (***2f***). **2f** obtained according to general protocol A from **3f** (6.1 g, 26.3 mmol), $POCl_3$ (4.9 mL, 52.6 mmol) and DMF (20 mL). Yield: 5.7 g (83%). ^{1}H NMR ($CDCl_3$): δ(ppm) 9.76 (s, 1H), 7.75 (d, J = 8 Hz, 2H), 7 (d, J = 8 Hz, 2H), 3.75 (m, 8H). ^{13}C NMR ($CDCl_3$): δ(ppm) 190.2, 151.3, 132.3, 126.6, 111.5, 50.6, 48.7. IR (KCl, cm^{-1}) 2102 (νN_3), 1673. Anal. Calcd for $C_{11}H_{13}N_7O$: C, 50.96; H, 5.05; N, 37.82. Found: C, 51.30; H, 5.42; N, 35.40. HR-MS (ES$^+$): [M + H]$^+$ 260.1266 (calcd 260.1260).

4-((2-Chloroethyl)(ethyl)amino)benzaldehyde (***2g***). Under argon, *N*-Ethyl-*N*-hydroxyethylaniline (4.2 mL, 26.3 mmol, 1 equiv.) was dissolved in dry DMF (20 mL, 0.26 mol, 10 equiv.), and the solution was cooled to 0 °C with an ice bath. $POCl_3$ (4.9 mL, 52.6 mmol, 2 equiv) was added slowly. After stirring at 40 °C for 8 h, the green solution was added in ice water and neutralized with solid K_2CO_3. The aqueous layer was extracted three times with CH_2Cl_2 (3 × 10 mL) and the combined organic phases were washed three times with water (3 × 10 mL), once with brine(10 mL), dried over sodium sulfate and concentrated under reduced pressure to afford pure yellow oil. Yield: 5.5 g (98%). ^{1}H NMR ($CDCl_3$): δ(ppm) 9.88 (s, 1H), 7.88 (d, J = 9 Hz, 2H), 6.9 (d, J = 9 Hz, 2H), 3.86 (m, 4H), 3.68 (q, J = 7.1 Hz, 2H), 1.38 (t, J = 7.1 Hz, 3H). ^{13}C NMR ($CDCl_3$): δ(ppm) 189.6, 151.4, 131.8, 125.3, 110.6, 51.6, 45.3, 39.8, 11.9. IR (KCl, cm^{-1}) 1666, 1240. Anal. Calcd for $C_{11}H_{14}NClO$: C, 62.41; H, 6.67; N, 6.62. Found: C, 62.14; H, 6.79; N, 6.64. HR-MS (ES$^+$): [M + Na]$^+$ 234.0659 (calcd 234.0662).

4-(Bis(2-chloroethyl)amino)benzaldehyde (***2h***). was synthesized accordingly starting from *N*-Phenyldiethanolamine (4.7 g, 26.3 mmol, 1 equiv.), dry DMF (20 mL, 0.26 mol, 10 equiv.) and $POCl_3$((7.4 mL, 78.9 mmol, 3 equiv.). Brown solid 6.28 g (97%). ^{1}H NMR ($CDCl_3$): δ(ppm) 9.88 (s, 1H), 7.87 (d, J = 8.9 Hz, 2H), 6.85 (d, J = 8.9 Hz, 2H), 3.87 (m, 8H). ^{13}C NMR ($CDCl_3$): δ(ppm) 190.1, 132.2, 111.6, 102.2, 98.2, 54.2, 40.5. IR (KCl, cm^{-1}) 1668, 1240. Anal. Calcd for ($C_{11}H_{13}NCl_2O$): C, 53.68; H, 5.32; N, 5.69. Found: C, 53.62; H, 5.44; N, 5.72. HRSM (ES$^+$): [M + Na]$^+$ 246.0445 (calcd 246.0452). m.p.(heptane): 87 °C.

(*E*)-*2*-(*3*-(*4*-(*Diethylamino*)*styryl*)-*5,5-dimethylcyclohex-2-enylidene*)*malononitrile* (***1a***). **1a** was obtained according to general protocol B from 4-diethylaminobenzaldehyde (1.77 g, 10 mmol) and **4** (1.86 g, 10 mmol). After concentration, the resulting oil was dissolved in water (50 mL) and extracted with dichloromethane (3 × 50 mL). The combined organic phases were dried with Na_2SO_4, filtered and evaporated. The black solid was crystallized from toluene. Yield 2 g (57%), dark solid. ^{1}H NMR ($CDCl_3$): δ 7.38 (d, 2H, J = 8.96 Hz), 7.01 (d, 1H, J_{trans} = 16 Hz), 6.76 (d, 1H, J_{trans} = 16 Hz), 6.73 (s, 1H), 6.64 (d, 2H, J = 8.96 Hz), 3.41 (q, 4H, 7.02 Hz), 2.56 (s, 2H), 2.44 (s, 2H) 1.20 (t, 6H, J = 7.02 Hz), 1.06 (s, 6H). ^{13}C NMR ($CDCl_3$): δ 169.1, 155.4, 149.1, 138.3, 129.7, 123.7, 122.7, 121.0, 114.3, 113.5, 111.5, 77.2, 44.5, 42.9, 39.2, 31.9, 28.0, 12.6. IR (KCl, cm^{-1}) 2223 (ν_{CN}). Anal. Calcd for $C_{23}H_{27}N_3$: C, 79.96; H, 7.88; N, 12.16. Found: C, 80.01; H, 7.85; N, 12.04. mp (toluene): 169−171 °C.

(*S,E*)-*2*-(*3*-(*4*-(*Ethyl*(*1-phenylethyl*)*amino*)*styryl*)-*5,5-dimethylcyclohex-2-enylidene*)*malononitrile* (***1b***). **1b** was obtained according to general protocol B from **2b** (150 mg, 0.5 mmol.) and **4** (93 mg, 0.5 mmol.). The product is purified by chromatography on silica, eluting with chloroform. Yield 60 mg (24%), deep red solid. ^{1}H NMR ($CDCl_3$): δ 7.39 (d, J = 9 Hz, 2H), 7.33 (t, J = 9 Hz, 2H), 7.27 (m, 3H), 7 (d, J = 16 Hz, 1H), 6.78 (m, 3H), 6.74 (s, 1H), 5.19 (q, J = 7 Hz, 1H), 3.31 (m, 2H), 2.57 (s, 2H), 2.44 (s, 2H), 1.65 (d, J = 7 Hz, 3H), 1.11 (t, J = 7 Hz, 3H), 1.06 (s, 6H). ^{13}C NMR ($CDCl_3$): δ 169.3, 155.4, 150.015, 142.1, 138.2, 129.7, 128.7, 127.3, 127, 124.4, 123.7, 121.5, 114.4, 113.6, 112.9, 75.8, 56.3, 43.2, 40.5, 32.4, 39.4, 32.1, 31, 28.2, 17.9. IR (KCl, cm^{-1}) 2215 (ν_{CN}). Anal. Calcd for $C_{29}H_{31}N_3$: C, 82.62; H, 7.41; N, 9.97. Found: C, 81.44; H, 7.35; N, 9.81. m.p.: 133−135 °C.

(±,*E*)-*2*-(*3*-(*4*-(*Hexyl*(*1-phenylethyl*)*amino*)*styryl*)-*5,5-dimethylcyclohex-2-enylidene*)*malononitrile* (***1c***). Obtained according to general protocol B from **2c** (154 mg, 0.5 mmol.), **4** (93 mg, 0.5 mmol.). The product is purified by chromatography on silica, eluting with chloroform. Yield 125 mg (52%). ^{1}H NMR ($CDCl_3$): δ 7.38 (d, J = 9 Hz, 2H), 7.33 (t, J = 9 Hz, 2H), 7.27 (m, 3H), 7 (d, J = 16 Hz, 1H), 6.79 (d, J = 16 Hz, 1H), 6.73 (m, 3H), 5.18 (q, J = 7 Hz, 1H), 3.17 (m, 2H), 2.56 (s, 2H), 2.44 (s, 2H), 1.64 (d, J = 7 Hz, 3H), 1.5 (m, 2H), 1.23 (m, 6H), 1.06 (s, 6H), 0.86 (t, J = 7 Hz, 3H). δ(ppm) 170.5, 169.3, 159.8, 155.4, 150.3, 142, 138.2, 129.7, 128.7, 127.3, 127.1, 124.3, 123.7, 121.5, 120.7, 114.4, 113.6, 113.1, 75.8, 56.6, 45.8, 46.6, 43.2, 42.8, 39.4, 32.1, 28.2, 27.9, 27.1, 26.9, 25.4, 22.7, 17.9, 14.1. IR (KCl, cm^{-1}) 2223 (ν_{CN}). Anal. Calcd for $C_{23}H_{27}N_3$: C, 82.97; H, 8.23; N, 8.80. Found: C, 81.18; H, 8.11; N, 9.81.

(*E*)-*2*-(*3*-(*4*-(*Diphenylamino*)*styryl*)-*5,5-dimethylcyclohex-2-enylidene*)*malononitrile* (***1d***). Obtained according to general protocol B starting from **3d** (3.77 g, 13.8 mmol) and **4** (2.6 g, 13.8 mmol). After removal of the solvents, the product was purified by chromatography eluting with CH_2Cl_2 to give a red solid. Yield: 4.7 g (77%). ^{1}H NMR (Acetone-d6): δ 7.59 (d, 2H, J = 10 Hz), 7.25 (m, 12H), 6.97 (d, 2H, J = 10 Hz), 6.82 (s, 1H), 2.65 (s, 2H), 2.61 (s, 2H), 1.1 (s, 6H). ^{13}C NMR (Acetone-d6): δ(ppm) 170.4, 162.9, 156.4, 150.1, 147.8, 138.1, 130.5, 129.9, 128.1, 126.2, 125, 123, 122.5, 43.4, 39.4, 32.5, 28. IR (KCl, cm^{-1}) 2215 (ν_{CN}). Anal. Calcd for $C_{31}H_{27}N_3$: C, 84.32; H, 6.16; N, 9.52. Found: C, 82.08; H, 6.31; N, 11.63. HR-MS (ES$^+$): M$^{+\circ}$ 441.2212 (calcd. 441.2205). m.p.(dichloromethane-cyclohexane): 128 °C.

(*E*)-*2*-(*3*-(*4*-((*2-Azidoethyl*)(*ethyl*)*amino*)*styryl*)-*5,5-dimethylcyclohex-2-enylidene*)*malononitrile* (***1e***). **1e** was obtained according to general protocol B from **3e** (3 g, 13.8 mmol) and **4** (2.6 g, 13.8 mmol). The mixture was crystallized at −20 °C from a toluene/pentane (1/1, v/v) mixture, filtered, and dried under a vacuum to afford pure red solid. Yield: 4.9 g (92%). ^{1}H NMR

(acetone-d6): δ(ppm) 7.57 (d, J = 10 Hz, 2H), 7.25 (d, J_{trans} = 16 Hz, 1H), 7.09 (d, J_{trans} = 16 Hz, 1H), 6.83 (d, J = 10 Hz, 2H), 6.74 (s, 1H), 3.61 (m, 6H), 2.61 (s, 2H), 2.58 (s, 2H). ^{13}C NMR (acetone-d6): δ(ppm) 170.3, 157.3, 150, 139.4, 130.7, 125.3, 121.7, 114.9, 114.2, 112.9, 75.7, 49.8, 45.8, 12.8. IR (KCl, cm^{-1}) 2215 (ν_{CN}), 2092 (νN_3). Anal. Calcd for $C_{23}H_{26}N_6$: C, 71.48; H, 6.78; N, 21.74. Found: C, 71.38; H, 6.75; N, 21.80. HR-MS (ES$^+$): MH$^+$ 387.2301 (calcd 387.2297). m.p.(toluene-pentane): 121 °C.

(*E*)-*2*-(*3*-(*4*-(*Bis*(*2-azidoethyl*)*amino*)*styryl*)-*5,5-dimethylcyclohex-2-enylidene*)*malononitrile* (***1f***). was obtained according to general protocol B from **3f** (3 g, 13.8 mmol) and **4** (2.6 g, 13.8 mmol). The mixture was crystallized at −20 °C from a toluene/pentane (1/1, v/v) mixture, filtered and dried under a vacuum to afford pure red solid. Yield: 5.3 g (89%). ^{1}H NMR (Acetone-d6): δ(ppm) 7.6 (d, J = 10 Hz, 2H), 7.28 (d, J_{trans} = 16 Hz, 1H), 7.13 (d, J_{trans} = 16 Hz, 1H), 6.91 (d, J = 10 Hz, 2H), 6.77 (s, 1H), 3.7 (m, 8H), 2.63 (s, 2H), 2.6 (s, 2H). ^{13}C NMR (Acetone-d6): δ(ppm) 170.3, 157.1, 145.6, 139.1, 130.7, 125.9, 122, 113.3, 50.7, 49.5, 43.4, 39.5, 32.5, 28. IR (KCl, cm^{-1}) 2215 (ν_{CN}), 2096 (νN_3). Anal. Calcd for $C_{23}H_{25}N_9$: C, 64.62; H, 5.89; N, 29.49. Found: C, 63.16; H, 5.87; N, 26.93. HR-MS (ES$^+$): MNa$^+$ 450.2142 (calcd 450.2131). mp (toluene/pentane): 165 °C.

(*E*)-*2*-(*3*-(*4*-((*2-Chloroethyl*)(*ethyl*)*amino*)*styryl*)-*5,5-dimethylcyclohex-2-enylidene*)*malononitrile* (***1g***). **1g** was obtained according to general protocol B from **3g** (2.9 g, 13.8 mmol) and **4** (2.6 g, 13.8 mmol). The mixture was precipitated in an ethanol/water mixture (1/1, v/v), filtered, and dried under a vacuum to afford pure dark red solid. Yield: 4.8 g (91%). ^{1}H NMR (CD_2Cl_2): δ(ppm) 7.42 (d, J = 9.9 Hz, 2H), 7.04 (d, J = 14.9 Hz, 1H), 6.86 (d, J = 14.9 Hz, 1H), 6.76 (s, 1H), 6.7 (d, J = 9.9 Hz, 2H), 3.67 (m, 4H), 3.48 (q, J = 7.5 Hz, 2H), 2.58 (s, 2H), 2.47 (s, 2H), 1.2 (t, J = 7.5 Hz, 3H), 1.06 (s, 6H). ^{13}C NMR (CD_2Cl_2): δ(ppm) 169.9, 155.9, 149.1, 141.9, 138.3, 130.2, 125.2, 122.1, 114, 112.4, 52.6, 46.1, 43.5, 41.1, 39.7, 32.4, 28.3, 12.8. IR (KCl, cm^{-1}) 2219 (ν_{CN}). Anal. Calcd for $C_{23}H_{26}N_3Cl$: C, 72.71; H, 6.9; N, 11.06. Found: C, 73.00; H, 7.08; N, 11.39. HR-MS (ES$^+$): MH$^+$ 380.1893 (calcd 380.1894). mp (ethanol/water): 185 °C.

(*E*)-*2*-(*3*-(*4*-(*Bis*(*2-chloroethyl*)*amino*)*styryl*)-*5,5-dimethylcyclohex-2-enylidene*)*malononitrile* (***1h***). **1h** was obtained according to general protocol B from **3g** (3.4 g, 13.8 mmol) and **4** (2.6 g, 13.8 mmol). The mixture was precipitated in an ethanol/water mixture (1/1, v/v), filtered, and dried under a vacuum to afford pure dark red solid. Yield: 5.2 g (90%). ^{1}H NMR (CD_2Cl_2): δ(ppm) 7.45 (d, J = 8 Hz, 2H), 7.05 (d, J_{trans} = 16 Hz, 1H), 6.87 (d, J_{trans} = 16 Hz, 1H), 6.77 (s, 1H), 6.72 (d, J = 8 Hz, 2H), 3.74 (m, 8H), 2.58 (s, 2H), 2.47 (s, 2H), 1.06 (s, 6H). ^{13}C NMR (Acetone-d6): δ(ppm) 171.2, 157, 138.9, 130.7, 129.8, 126.1, 122.1, 113.1, 53.5, 43.4, 41.5, 39.5, 28. IR (KCl, cm^{-1}) 2217 (ν_{CN}). Anal. Calcd for $C_{23}H_{25}N_3Cl_2$: C, 66.67; H, 6.08; N, 10.14. Found: C, 66.71; H, 6.24; N, 10.3. HRSM (ES$^+$): MH$^+$ 414.1497 (calcd 414.1504). mp (ethanol - water): 178 °C.

(*E*)-*2,2′*-(*4*-(*2*-(*3-Dicyanomethylene*)-*5,5-dimethylcyclohex-1-enyl*)-*vinyl*)*phenylazanediyl*)*bis*(*ethane*)*bis*(*ethane-2,1-diyl*)*diacetate* (***1i***). **1i** was obtained according to general protocol B from **2i** (2.5 g, 8.52 mmol) and **4** (1.58 g, 8.52 mmol). The product was purified by chromatography on silica eluting with dichloromethane. Yield: 3.53 g (90%). ^{1}H NMR ($CDCl_3$): δ(ppm) 7.4 (d, J = 9 Hz, 2H), 6.99 (d, J = 16 Hz, 1H), 6.8 (d, J = 16 Hz, 1H), 6.75 (m, 3H), 4.26 (t, J = 6 Hz, 4H), 3.67 (t, J = 6 Hz, 4H), 2.56 (s, 2H), 2.44 (s, 2H), 2.05 (s, 6H), 1.06 (s, 6H). ^{13}C NMR ($CDCl_3$): δ(ppm) 170.9, 169.3, 155.1, 148.8, 137.7, 129.7, 125.1, 124.7, 121.9, 114.2, 113.4, 112.2, 76.4, 61.3, 49.7, 43.1, 39.4, 32.1, 28.1, 20.9. Anal. Calcd for $C_{23}H_{27}N_3$: C, 82.97; H, 8.23; N, 8.80. Found: C, 81.18; H, 8.11; N, 9.81.

Acknowledgment. The authors thank the Région Rhône-Alpes (cluster 5) for a grant to J.M. and financial support.

Supporting Information Available: Spectroscopic data for all compounds **1a**−**1i** (PDF) and crystallographic information (CIF). This material is available free of charge via the Internet at http://pubs.acs.org.